

Energy dependence of hard bremsstrahlung production in proton-proton collisions in the $\Delta(1232)$ region

D. Tsirkov¹, V. Komarov¹, T. Azaryan¹, D. Chiladze^{2,3},
 S. Dymov^{1,4}, A. Dzyuba⁵, M. Hartmann², A. Kacharava²,
 A. Khoukaz⁶, A. Kulikov¹, V. Kurbatov¹, G. Macharashvili^{1,3},
 S. Merzliakov^{1,2}, M. Mielke⁶, S. Mikirtychiants^{2,5},
 M. Nekipelov², F. Rathmann², V. Serdyuk^{1,2}, H. Ströher²,
 Yu. Uzikov¹, Yu. Valdau^{2,5} and C. Wilkin⁷

¹ Laboratory of Nuclear Problems, Joint Institute for Nuclear Research, RU-141980 Dubna, Russia

² Institut für Kernphysik and Jülich Centre for Hadron Physics, Forschungszentrum Jülich, D-52425 Jülich, Germany

³ High Energy Physics Institute, Tbilisi State University, 0186 Tbilisi, Georgia

⁴ Physikalisches Institut II, Universität Erlangen-Nürnberg, D-91058 Erlangen, Germany

⁵ High Energy Physics Department, Petersburg Nuclear Physics Institute, RU-188350 Gatchina, Russia

⁶ Institut für Kernphysik, Universität Münster, D-48149 Münster, Germany

⁷ Physics and Astronomy Department, UCL, London, WC1E 6BT, United Kingdom

E-mail: cw@hep.ucl.ac.uk

Abstract. Hard bremsstrahlung production in proton-proton collisions has been studied with the ANKE spectrometer at COSY-Jülich in the energy range of 353–800 MeV by detecting the final proton pair $\{pp\}_s$ from the $pp \rightarrow \{pp\}_s \gamma$ reaction with very low excitation energy. Differential cross sections were measured at small diproton c.m. angles from 0° to 20° and the average over this angular interval reveals a broad peak at a beam energy around 650 MeV with a FWHM ≈ 220 MeV, suggesting the influence of $\Delta(1232)N$ intermediate states. Comparison with deuteron photodisintegration shows that the cross section for diproton production is up to two orders of magnitude smaller, due largely to differences in the selection rules.

PACS numbers: 25.40.Ep, 13.60.-r, 25.20.Dc

Submitted to: *J. Phys. G: Nucl. Phys.*

1. Introduction

The photodisintegration of the deuteron

$$\gamma d \rightarrow pn, \quad (1)$$

is the simplest reaction of its type and has therefore attracted much attention, both theoretical and experimental, to learn more about how to treat the interaction of the electromagnetic field with nuclei. Significant advances in the understanding of the dynamics at several hundred MeV have been achieved within the framework of models that are either perturbative, taking into account a set of relevant Feynman diagrams [1], or employ a coupled NN , $N\Delta$, $\Delta\Delta$ and $NN\gamma$ channel formalism [2, 3]. Nevertheless, extensive work on the reaction continues and a full interpretation of the data has still to be achieved [4].

A kinematically similar reaction involves the photodisintegration of a 1S_0 proton pair (diproton), here denoted by $\{pp\}_s$,

$$\gamma \{pp\}_s \rightarrow pp. \quad (2)$$

Reactions (1) and (2) share the common feature that, in the $\Delta(1232)$ range and above, there is a large energy transfer from the photon to the target nucleon pair, transforming it into one of high invariant mass and driving the final state deep into the nucleon resonance region [5]. Thus, in contrast to other electromagnetic processes, such as electron-deuteron elastic scattering, the nucleon resonance excitation channels are explicitly open. As a consequence, the influence of isobar or mesonic exchange currents is likely to be very strong for both reactions.

Since the diproton is the spin-isospin partner of the deuteron, reactions (1) and (2) involve different transitions. Whereas one of the main driving terms for $\gamma d \rightarrow pn$ is an $M1$ excitation of an S -wave $\Delta(1232)N$ pair that de-excites into pn , an analogous transition is forbidden by angular momentum and parity conservation for the $\gamma \{pp\}_s \rightarrow pp$ reaction [1]. There are likely to be cancellations among the large amplitudes as one approaches the pure S -wave diproton limit and this means that extra insight may be gained into the field through a combined study of the photodisintegration of the deuteron and diproton.

However, the free 1S_0 proton pair is not bound and the diproton investigation has generally been approached through the photodisintegration of a pp pair embedded in a light nucleus, in particular ${}^3\text{He}$. By studying events where there were two fast protons emerging from the $\gamma {}^3\text{He} \rightarrow ppn$ reaction with a slow (reconstructed) neutron, this part of phase space was primarily interpreted in terms of an interaction on a diproton, with the neutron merely appearing as a *spectator* particle, whose influence is only felt through the kinematics [6–14]. These data show little indication for the excitation of an intermediate $\Delta(1232)N$ state, certainly much less than for those for fast pn pairs [11, 12].

As pointed out in several of these publications, the corrections to the simple spectator model picture can be quite large, owing mainly to the fact that the photoabsorption on pn pairs is much stronger than on pp . This makes it harder to

separate cleanly these two terms, especially at the lower energies where the Dalitz plot is not sufficiently wide. Final state interactions, where the neutron from a fast pn pair undergoes a charge-exchange reaction on a spectator proton, and other three-body mechanisms have also to be considered.

In view of these potential drawbacks, it is well worth seeing if the information derived from these experiments could be complemented by a direct measurement of the cross section for

$$pp \rightarrow \{pp\}_s\gamma. \quad (3)$$

In order to ensure that the final diproton is almost exclusively in the 1S_0 state, it is crucial that the pp excitation energy E_{pp} be very small, and this is an important constraint on any measurement. For small E_{pp} , the proton beam energy T_p is essentially twice the photon energy E_γ for the inverse reaction.

There have been many measurements of bremsstrahlung in proton-proton scattering in the few hundred MeV range [15–20]. These were generally accomplished through the use of pairs of counters placed on either side of the primary beam direction. As a consequence they were not sensitive to the behaviour at low E_{pp} , i.e. to the hardest part of the bremsstrahlung spectrum. The one early exception benefitted from the wide acceptance offered by the COSY-TOF spectrometer, where data were taken at 293 MeV [21]. However, the statistics in the low E_{pp} region were severely limited and a cross section for this region was not given.

The first data on hard bremsstrahlung production in reaction (3) at intermediate energies were reported recently from an experiment carried out at the ANKE facility at the Cooler Synchrotron COSY-Jülich [22]. The $pp \rightarrow \{pp\}_s\gamma$ differential cross section was measured at energies $T_p = 353, 500$ and 550 MeV. Events were here selected with a final excitation energy $E_{pp} < 3$ MeV, where it is expected that the contribution from P -waves in the diproton should be minimised. However, due to the limited angular coverage of the forward detector employed in these studies, only small diproton c.m. angles θ_{pp} were covered; $0^\circ < \theta_{pp} < 20^\circ$. Since the cross section is symmetric about 90° , this effectively means a similar cut on the photon angle θ_γ ; $0^\circ < \theta_\gamma < 20^\circ$. In contrast, the full $pp \rightarrow \{pp\}_s\gamma$ angular domain was measured in a high statistics experiment at CELSIUS with the same E_{pp} cut [23], though only at the single (lower) energy of 310 MeV.

Taken together, the ANKE and CELSIUS data show a rise in the near-forward cross section from 310 to 550 MeV, but data at higher energy are needed to see if there is a maximum in the region of the $\Delta(1232)N$ threshold. To clarify the experimental situation, we have supplemented the earlier COSY-ANKE data [22] by measurements of the small angle $pp \rightarrow \{pp\}_s\gamma$ differential cross section at $T_p = 625, 700$ and 800 MeV. Combining the data sets allows us to study the energy dependence of the near-forward cross section throughout the $\Delta(1232)$ resonance region. Unlike some of the ${}^3\text{He}$ photodisintegration results [11, 12], our data reveal a significant maximum in a region where $\Delta(1232)N$ intermediate states might be expected to play a role and this

should provide a useful guide for further theoretical work.

In view of earlier publications, the description of the experiment and its analysis in section 2 could be made more brief. The results and their significance are discussed in section 3, with our conclusions and suggestions for further work being presented in section 4.

2. Measurement and Analysis

The experiment was carried out using the magnetic spectrometer ANKE [24], which is installed at an internal target station of COSY. A hydrogen cluster-jet target was positioned in the proton beam and the secondary particles were detected with wire chambers and a scintillation hodoscope. The three-momenta and trajectories of the particles were reconstructed on the basis of the known field map of the analysing magnet, assuming that these particles originated from a point-like source situated at the centre of the target-beam interaction volume.

The first step in the identification of the $pp\gamma$ final state was the selection of two coincident protons from among all the detected pairs of positively charged particles. The scintillation hodoscope allowed the measurement of the difference between the times of flight from the target to the detector for the two recorded particles. The comparison of this value with that *calculated* from the measured particle momenta and trajectories led to a very good identification of proton pairs, as illustrated in figure 1. The background from misidentified pairs was at the few percent level for all beam energies, as detailed in Table 1. Having identified two protons and determined their momenta, the complete kinematics of the $pp \rightarrow ppX$ process could be reconstructed. Events with zero missing mass, within the experimental resolution, were accepted as candidates for the $pp \rightarrow pp\gamma$ reaction. Those where the pair's kinetic energy E_{pp} in their rest frame is small, specifically $E_{pp} < 3$ MeV, were classified as belonging to reaction (3).

The experimental techniques, conditions of the measurements, and the data-handling procedure have been described in an earlier publication [22] and initial results given there at 353, 500, and 550 MeV. The new results at energies of 625, 700 and 800 MeV were obtained in three separate beam periods. As a consequence, there were some differences in the adjustment of the magnetic system setup and the number of sensitive planes in the tracking detector. The 625 and 800 MeV data were collected as by-products of the study of other reactions so that the measurement conditions were not optimised for the study of the $pp \rightarrow pp\gamma$ reaction. The data at 700 MeV were obtained with a polarised proton beam and a weighted average was then taken over the two polarisation states.

In order to measure the excitation energy of the proton pair and study the angular dependence of the cross section of the $pp \rightarrow pp\gamma$ reaction, sufficient resolution in the corresponding variables is needed. The uncertainty $\sigma(\theta_{pp})$ in the polar angle θ_{pp} of the diproton in the overall c.m. system ranged from 0.5° to 2.3° , depending on the

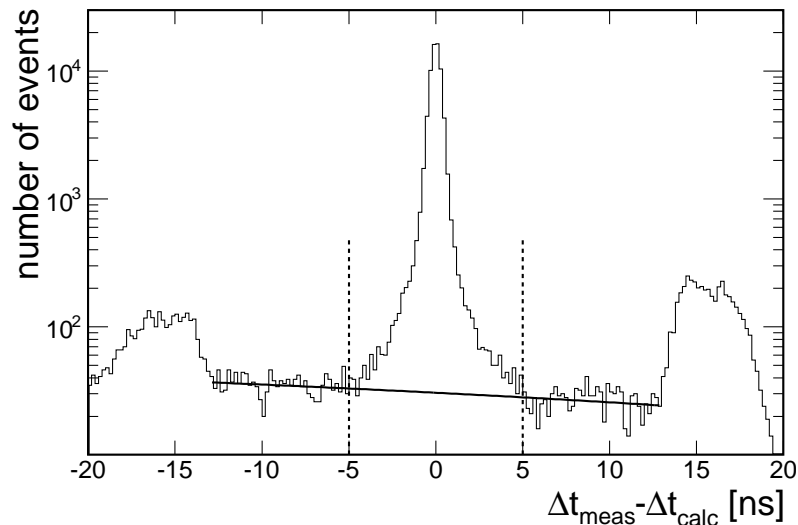


Figure 1. Identification of the proton pairs from the $pp \rightarrow ppX$ reaction on the basis of time-of-flight information at 700 MeV. Δt_{meas} is the directly measured difference of the times of flight; Δt_{calc} is the time-of-flight difference calculated using the measured particle momenta and trajectories. The central peak corresponds to proton pairs, whereas those around ± 15 ns are associated with $p\pi^+$ pairs. The full line is a linear approximation to the background arising from accidental coincidences. Events inside the indicated ± 5 ns interval were retained for the analysis.

Table 1. Characteristics of the measurements at different energies: integral luminosity L with systematic (first) and normalisation (second) errors; background/signal ratio N_{bg}/N_{pp} for proton pair identification; width $\text{FWHM}(M_\pi^2)$ of the π^0 peak in the missing-mass-squared distribution from the $pp \rightarrow \{pp\}_s X$ reaction. The reasons for the broader widths at 625 and 800 MeV are discussed in the text.

T_p (MeV)	L (10^{31}cm^{-2})	N_{bg}/N_{pp}	$\text{FWHM}(M_\pi^2) \times 10^{-3}$ ($(\text{GeV}/c^2)^2$)
353	$573 \pm 18 \pm 17$	4%	4.1
500	$331 \pm 10 \pm 13$	5%	6.3
550	$318 \pm 21 \pm 13$	4%	7.4
625	$46 \pm 1 \pm 2$	1.6%	15.8
700	$159 \pm 3 \pm 8$	2.2%	9.3
800	$67 \pm 1 \pm 3$	1.6%	18.9

beam energy and the value of θ_{pp} . The uncertainty in the excitation energy E_{pp} , which generally increased with E_{pp} , was between 0.08 to 0.6 MeV for $E_{pp} < 3$ MeV, depending also on the beam energy. The E_{pp} resolution was thus sufficient for the measurement of the excitation energy spectra up to 3 MeV. The E_{pp} spectra for $pp \rightarrow \{pp\}_s \gamma$, as well as for the $pp \rightarrow \{pp\}_s \pi^0$ reaction, are satisfactorily reproduced by Monte Carlo simulations, where events were generated according to phase space modified by the S -wave pp final state interaction [22, 25]. Extra evidence for the S -wave nature of the proton pairs was provided by the isotropy of the acceptance-corrected angular distributions in the

diproton rest frame.

The distributions in missing mass squared M_x^2 for events where $\theta_{pp} < 20^\circ$ are shown in figure 2 for the six beam energies. At 353 MeV there is a clear γ peak that is well separated from the pion peak associated with the $pp \rightarrow \{pp\}_s \pi^0$ reaction. The low background arising from accidental proton coincidences changes weakly with M_x^2 and could be taken as linear in the interval $-0.02 < M_x^2 < +0.06$ (GeV/c^2)².

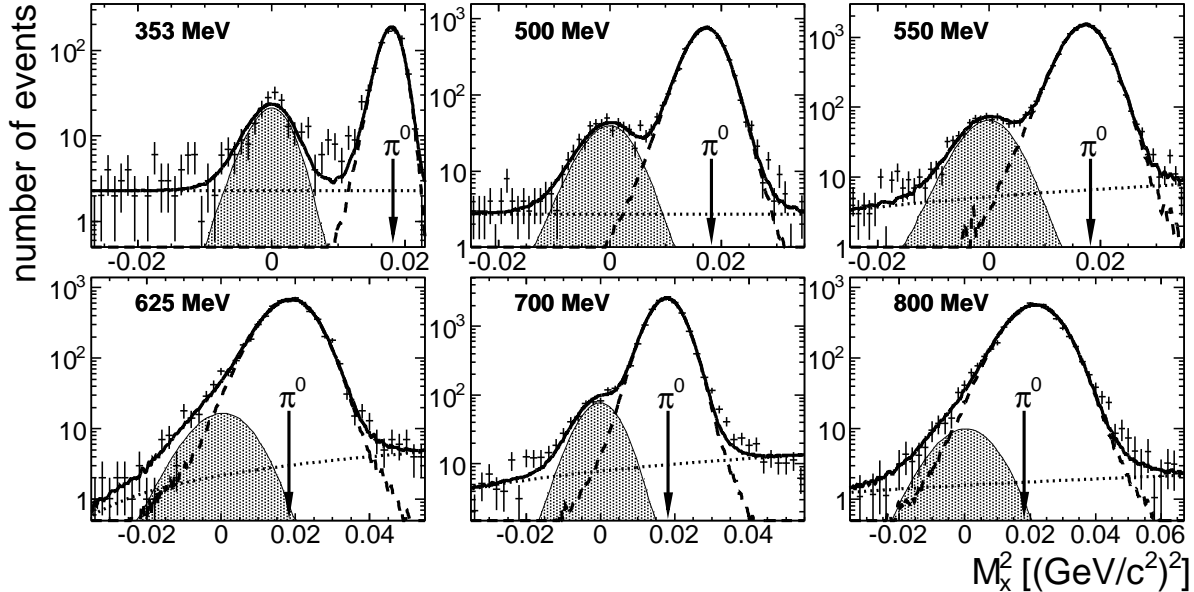


Figure 2. Distributions of the missing mass squared in the $pp \rightarrow \{pp\}_s X$ reaction for proton pairs with $\theta_{pp} < 20^\circ$ compared to fits with different contributions. The expected π^0 position is indicated by the arrow. The shaded area corresponds to the γ peak, the dashed line to the π^0 peak, the dotted to the linear accidental background, and the solid to the sum of these three contributions. The data at the three lower energies were reported in [22], whereas the others are from this work.

The widths of the peaks in figure 2 are governed by the accuracy of the measurement of the proton three-momenta in the relevant experimental runs and this generally gets worse with increasing beam energy. The corresponding growth in the widths reported in Table 1 results at higher energies in the merging of the γ signal with that of the pion. The principal difficulty consists therefore in selecting the small number of γ events from the total distribution.

The M_x^2 distributions were fitted by a sum of peaks, corresponding to γ and π^0 production, plus a linear background. In order to estimate the shapes of the peaks as reliably as possible, a detailed Monte-Carlo simulation was undertaken at each energy, taking into account all the known features of the setup. These include, in particular, the smearing caused by the radial distribution of the proton beam at the target region, the multiple scattering in the exit window of the vacuum chamber and detector materials, and the actual clustering of the wires fired in the proportional chambers. The procedure of track reconstruction used in the simulation was the same as that in the data handling.

The free parameters of interest used to fit the missing-mass spectra were the number of events in the γ peak, the number of events in the pion peak, and the two constants of the linear background. However, in order to compensate for the lack of knowledge of the beam spatial distribution, additional parameters were inserted into the fits. These were the shift of the pion peak position and correction factors for the γ and pion peak widths.

In order to investigate the systematics, several fitting methods were employed. Either both peaks were fitted together or the pion peak with the background was first fitted separately, excluding the M_x^2 range where the γ signal was expected. The correction for the setup acceptance was also accounted for in two different ways. This was either introduced for each event and the weighted M_x^2 spectrum fitted, or the uncorrected distribution was fitted and the number of γ events corrected for the average acceptance factor afterwards. Finally, two fitting approaches were tried, namely χ^2 minimisation and logarithmic likelihood, though the latter was used only for fitting uncorrected spectra. Although these techniques were developed primarily in order to identify the γ signal in the more difficult high energy cases, they were also used on the published data [22], but any changes there are of little significance.

At each energy the results obtained using the different methods were completely compatible and their average was taken, with the variation in the deduced cross section being considered as a systematic uncertainty. As a further check on the reliability of the identification of the γ signal in the most complicated cases of higher T_p , the M_x^2 distributions were also fitted assuming that there were no γ events. In this case the π^0 peak was first fitted, excluding the γ range around $M_x^2 = 0$, and the χ^2 of the difference between the resulting function and the histogram evaluated over the previously excluded γ range. The results of fitting the data at 625, 700 and 800 MeV with and without the γ contribution are shown in figure 3, where it is seen that, unless the γ is included, there is a significant deterioration in the values of χ^2 evaluated for the γ peak region even in the most severe case of 800 MeV.

The luminosity L was determined from the number of the elastically scattered protons detected in parallel. In order to correct for the acceptance, a simulation was carried out where the setup geometry, the efficiency of the proton detection by the multiwire proportional chambers, and the track reconstruction algorithm were taken into account. These measurements were then compared to differential cross sections predicted by the SAID analysis program [26]. Although this does not yield errors, study of experimental data in the literature suggests that the uncertainties range from about 3% at 353 MeV up to 5% at 800 MeV. Small variations of the luminosity (those exceeding the statistical fluctuations), derived at different proton angles, reflect uncertainty in the acceptance correction and were taken as systematic errors in the luminosity.

The total uncertainty was estimated as the quadratic sum of the statistical, systematic, and normalisation errors. As a general rule, statistical errors had a negligible effect so that they are not shown in Table 1. Also negligible is the contribution arising from the systematic error in the proton momentum.

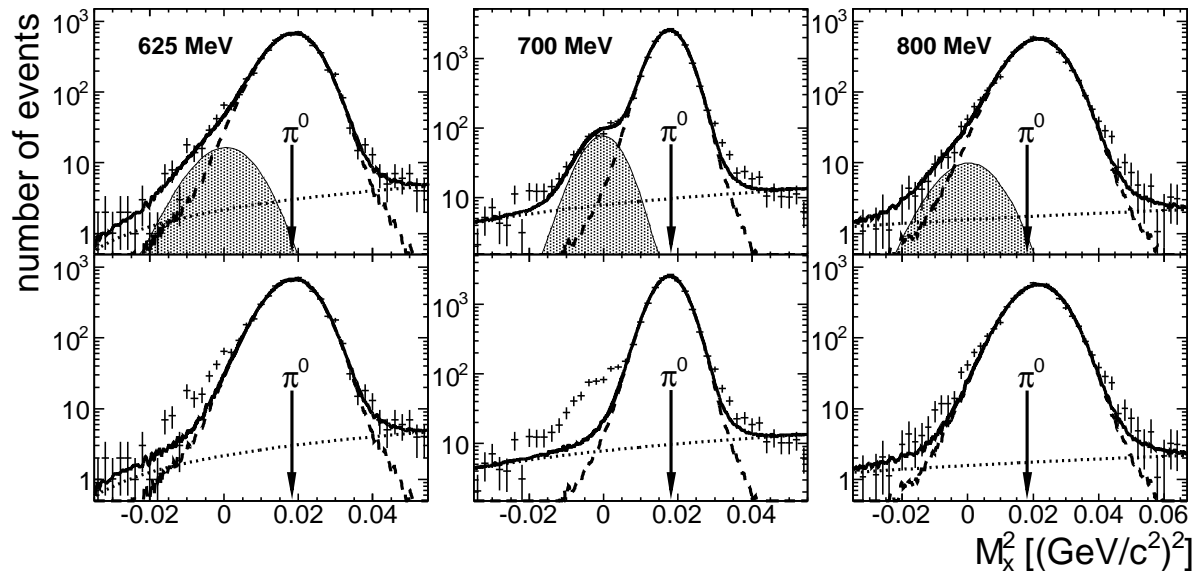


Figure 3. Descriptions of the M_x^2 distributions at 625, 700 and 800 MeV, assuming the presence (upper panels) or absence (lower panels) of a γ contribution, as explained in the text. The notation is as in figure 2. The values χ^2 per degree of freedom in the γ peak region increase significantly for fits that do not include the possibility of a γ signal. At 625 MeV the χ^2/ndf goes from 20.8/9 to 69.8/10, at 700 MeV from 9.7/9 to 314/10, and at 800 MeV from 9.7/9 to 36/10.

The angular dependences at 353, 500 and 550 MeV were reported earlier [22]. The poorer conditions did not allow similar studies to be made at 625 and 800 MeV. However, to estimate the angular dependence of the differential cross section at 700 MeV, we have divided the events into three θ_{pp} intervals, 0° – 7° , 7° – 12° , 12° – 20° , and made separate fits for each of these ranges.

3. Results and Discussion

In order to study the energy dependence of the $pp \rightarrow \{pp\}_s \gamma$ reaction from 353 to 800 MeV, we have evaluated the differential cross section $d\sigma/d\Omega_{(0-20)}$ averaged over the interval $0^\circ - 20^\circ$ in diproton c.m. angle. Our measurements show that the angular dependence is rather smooth in this region [22] so that the average cross section should reflect reasonably well the energy dependence at fixed angle.

The numbers of selected γ events, N_{raw} , and the corresponding acceptance-corrected figure, N_{corr} , are given in Table 2 for the six energies. Also to be found there are the average cross sections $d\sigma/d\Omega_{(0-20)}$, together with the corresponding partial and total errors. The uncertainties are particularly large at 625 and 800 MeV, due to the low luminosity and non-optimal conditions that hampered the identification of the γ signal.

As previously remarked, it was also possible to extract information on the angular dependence of the $pp \rightarrow \{pp\}_s \gamma$ reaction at 700 MeV by dividing the ANKE range into

Table 2. Numbers of $pp \rightarrow \{pp\}_s\gamma$ events and the corresponding differential cross sections at different beam energies. Data at 353, 500, and 550 MeV were already presented in [22]. Here N_{raw} is the number of registered $\{pp\}_s\gamma$ events, N_{corr} the number of events corrected for acceptance, and $d\sigma/d\Omega_{(0-20)}$ the differential cross section averaged over $0^\circ - 20^\circ$. The statistical error is denoted by σ_{stat} , that coming from the systematics in the γ event acquisition by σ_γ , and that arising from the luminosity uncertainty by σ_{lum} . Adding these contributions quadratically gives a total error of σ_{tot} .

T_p (MeV)	353	500	550	625	700	800
N_{raw}	180	335	525	177	450	114
N_{corr}	1126	2164	3722	810	2296	459
$d\sigma/d\Omega_{(0-20)}$ (nb/sr)	5.1	17.9	33.5	46.5	37.9	17.0
σ_{stat} , nb/sr	0.4	1.0	1.4	6.4	2.6	4.9
σ_γ , nb/sr	0.2	0.5	0.7	7.0	1.0	8.5
σ_{lum} , nb/sr	0.2	0.9	2.6	2.0	2.2	1.0
σ_{tot} , nb/sr	0.5	1.4	3.0	9.7	3.5	9.9

three intervals and the results are presented in Table 3. These data are compared in figure 4 with those obtained at lower energies [22]. Although the new data show some tendency for a forward dip, this is less strong than that measured at 500 and 550 MeV. In all cases, over the limited angular interval reported here, the cross section is consistent with a linear variation in $\cos^2 \theta_{pp}$.

Table 3. Angular dependence of the $pp \rightarrow \{pp\}_s\gamma$ reaction at 700 MeV.

θ_{pp}	$0^\circ-7^\circ$	$7^\circ-12^\circ$	$12^\circ-20^\circ$
$d\sigma/d\Omega$ (nb/sr)	34 ± 5	37 ± 4	42 ± 6

The measured values of the average cross section $d\sigma/d\Omega_{(0-20)}$ are shown in figure 5a as a function of the proton beam energy. Similar data are also available with the identical 3 MeV cut in E_{pp} at 310 MeV from CELSIUS [23]. Although this experiment had a much wider angular coverage, the value shown in the figure was obtained by taking the $0^\circ - 20^\circ$ average. This point joins very smoothly onto the ANKE data.

The energy dependence of the differential cross section of the $pp \rightarrow \{pp\}_s\gamma$ reaction shown in figure 5a reveals a broad peak, with a maximum near 650 MeV and FWHM ~ 220 MeV, and it is tempting to suggest that this might be associated in some way with the excitation of the $\Delta(1232)$ isobar. It is well known that this resonance plays a crucial role for the analogous $pn \rightarrow d\gamma$ reaction, whose energy dependence at a deuteron production angle of $\theta_d = 20^\circ$ with respect to the proton direction is also shown in the same figure, scaled down by a factor of twenty. These values were obtained from the MAMI deuteron photodisintegration $\gamma d \rightarrow np$ results [27] by using detailed balance.

It is important to note that the maximum in the $pp \rightarrow \{pp\}_s\gamma$ cross section appears

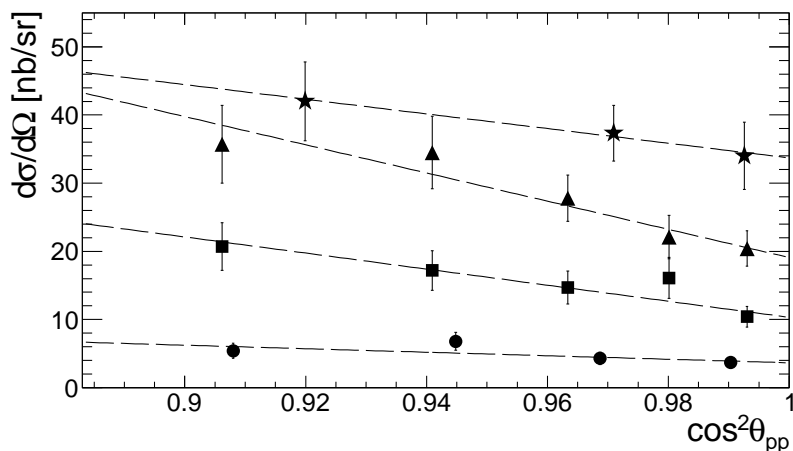


Figure 4. Angular dependence of the differential cross section for the $pp \rightarrow \{pp\}_s\gamma$ reaction at four beam energies. The results of the present measurement at 700 MeV are shown by stars. Also shown are the data from [22] at 353 MeV (circles), 500 MeV (squares), and 550 MeV (triangles). The errors coming from the statistics and background subtraction are shown but not the overall ones arising from the luminosity uncertainty. The lines represent linear fits to the four data sets.

at about 80 MeV higher than that for $pn \rightarrow d\gamma$. Direct excitation of the Δ -isobar dominates the $pn \rightarrow d\gamma$ reaction in this energy range through an $M1$ transition to an intermediate ΔN state in an S -wave. Such an $M1$ transition is forbidden in the diproton case [1] but the strength could come from a P -wave ΔN configuration, which requires extra energy in order to overcome the centrifugal barrier. Similar arguments have been used to explain why the Δ peak is shifted to higher energy also for the $pp \rightarrow \{pp\}_s\pi^0$ reaction [28]. In addition to the displacement of the $pp \rightarrow \{pp\}_s\gamma$ peak position to higher energies, it is narrowed significantly compared to $pn \rightarrow d\gamma$.

The ratio of the two differential cross sections

$$R = \frac{d\sigma/d\Omega(pn \rightarrow d\gamma)}{d\sigma/d\Omega(pp \rightarrow \{pp\}_s\gamma)} \quad (4)$$

is presented in figure 5b. Where necessary, the $pn \rightarrow d\gamma$ data [27] were spline-interpolated in energy. The smallest c.m. angle in these measurements was 20° and these are compared in the figure to the diproton results both at this angle and averaged between 0° and 20° .

What is striking about the ratio shown in figure 5b is the smallness of the diproton cross section compared to that for the deuteron. The factor is strongly energy dependent, dropping smoothly from over 100 at low energies to about 20 at 800 MeV. It should, however, be borne in mind that some of this suppression is to be associated with the difference in the phase space volume for producing the deuteron bound state and diproton continuum state.

The theoretical treatment of the $pp \rightarrow \{pp\}_s\gamma$ reaction has been far less developed than that for $pn \rightarrow d\gamma$. The first thing to note is that, in the diproton case, the $E1$ transition is suppressed by the vanishing of an electric dipole operator for the proton

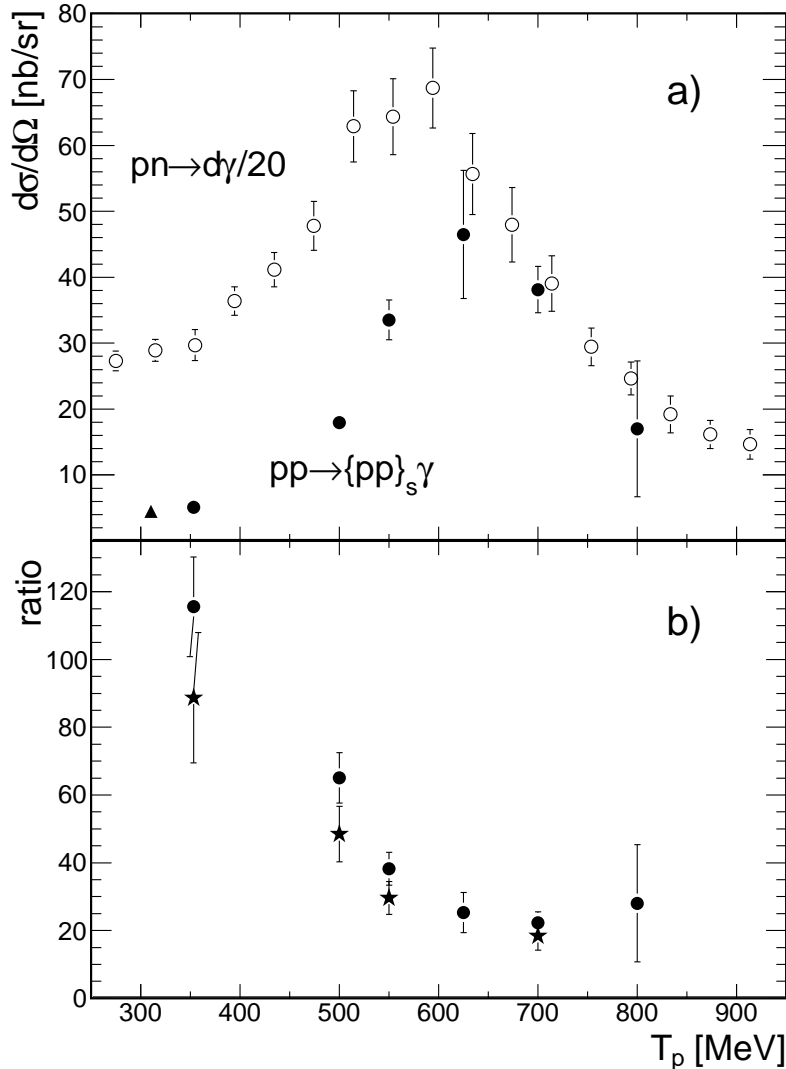


Figure 5. (a) Energy dependence of the $pp \rightarrow \{pp\}_s \gamma$ and $pn \rightarrow d\gamma$ differential cross sections. Full circles represent COSY-ANKE data for the average differential cross section $d\sigma/d\Omega_{(0-20)}$ for the $pp \rightarrow \{pp\}_s \gamma$ reaction whereas the triangle is taken from the CELSIUS results [23] for the same angular and E_{pp} conditions. The open circles show the values of the differential cross section for the $pn \rightarrow d\gamma$ reaction at a deuteron c.m. angle of $\theta_d = 20^\circ$ with respect to the proton direction, evaluated from the deuteron photodisintegration data of [27] and scaled down by a factor of twenty. (b) Ratio of the differential cross sections for $pn \rightarrow d\gamma$ to $pp \rightarrow \{pp\}_s \gamma$, as defined by equation (4). The stars were obtained for the same production angle $\theta_d = \theta_{pp} = 20^\circ$ while for the circles the angular average of the $pp \rightarrow \{pp\}_s \gamma$ cross section over $0^\circ - 20^\circ$ was used.

pair. The absence of charged pion exchange currents also reduces some of the meson exchange effects. Finally, because the S -wave $J^P = 1^+$ ΔN intermediate state cannot couple to an initial pp system [1], the $M1$ transition that dominates the $pn \rightarrow d\gamma$ reaction in the few hundred MeV region is also not present. One might therefore expect the first effects of the Δ degrees of freedom to show up in an S -wave $J^P = 2^+$ ΔN

contribution, which would lead to an $E2$ transition, or through a ΔN configuration in a P or higher wave. The coupled-channel calculations of [29] suggest that at intermediate energies the $E2$ multipole should dominate and this would give rise to a $\sin^2 \theta_\gamma \cos^2 \theta_\gamma$ dependence. In addition, this model showed no sign for any apparent ΔN signal in the energy variation, in contrast to our data. Furthermore, the CELSIUS data at 310 MeV show a linear variation with $\cos^2 \theta_\gamma$ so that any $E2$ contribution at this energy should be very small.

In a recent publication [30] the high precision KVI pp bremsstrahlung data at 190 MeV [19] have been successfully described for the first time through the introduction of a phenomenological contact interaction current that explicitly satisfies the generalised Ward-Takahashi identity. However, these data did not sample the hard bremsstrahlung limit. A generalisation of the theoretical model includes some Δ contributions, but it still neglects entirely the interaction current due to the Δ that gives rise to the five-point contact current [31]. It is not clear if this is the reason why it did not reproduce the shape of the angular distribution for small E_{pp} from CELSIUS at 310 MeV [23].

A peak in the energy dependence of the $pp \rightarrow \{pp\}_s \gamma$ differential cross section due to the ΔN configuration was obtained in calculations [32] within the framework of a simplified one-pion-exchange model. However, gauge invariance was not imposed and other terms neglected.

4. Summary and conclusions

The differential cross section for hard bremsstrahlung production in proton-proton collisions has been measured in the near-forward direction, $0^\circ - 20^\circ$, for beam energies between 353 and 800 MeV. The energy dependence of this cross section reveals a broad peak around 650 MeV, which is roughly where one might expect a contribution from a $\Delta(1232)N$ intermediate state. The peak is shifted to higher energies compared to that in the analogous $pn \rightarrow d\gamma$ reaction but this is not surprising because the S -wave $J^p = 1^+$ ΔN state that drives the $M1$ transition in the deuteron case does not couple to an initial pp system.

The suppression of the isobar $M1$ term leads to a large but energy-dependent factor between the cross sections for $pn \rightarrow d\gamma$ and $pp \rightarrow \{pp\}_s \gamma$. It also makes the theoretical description harder to realise because there is then no longer an obviously dominant term to consider. Further theoretical work is clearly needed.

Even with a 3 MeV cut in E_{pp} there might be some small contamination of P -waves in the pp system but there are similar concerns for the ${}^3\text{He}(\gamma, pp)n$ data because variational Monte Carlo calculations suggest that the pp pair in ${}^3\text{He}$ is not in a pure 1S_0 state and might also contain a few per cent of higher partial waves [33].

The combined study of the $pn \rightarrow d\gamma$ and $pp \rightarrow \{pp\}_s \gamma$ reactions has assumed a greater importance in recent years because of the interest in the investigation of short-range pn and pp correlations in nuclei [14, 34, 35]. These are studied through photoabsorption that leads to the emission of nucleon pairs with large back-to-back

momenta in the pair's rest frame.

On the experimental side, the separation of the various multipoles in the $pp \rightarrow \{pp\}_s \gamma$ reaction would clearly require the measurement of the cross section (and analysing power) over a wider angular region and this will be possible at ANKE through the use of a positive side detector in combination with the forward detector [36] that provided the data reported here. Of great use in the separation would be data on the proton-proton spin correlation parameters and it might be possible to study these at COSY-ANKE through the use of a polarised gas cell target [37].

New experimental data [14] has allowed the comparison of the cross sections for $d(\gamma, p)n$ and ${}^3\text{He}(\gamma, pp)n$ at $\theta_{\text{cm}} = 90^\circ$. These data come from the scaling energy region, $E_\gamma > 2.4$ GeV, where the influence of the additional nucleon in the ${}^3\text{He}$ target is of less importance. The ratio of the cross sections found there was ≈ 40 , but to compare with the R ratio of equation 4, one needs to transform data with a bound diproton to ones with a scattering pp system, which requires a model calculation.

An extension of the experimental study of the $pp \rightarrow \{pp\}_s \gamma$ reaction from the $\Delta(1232)$ excitation region to GeV energies could provide an alternative way to investigate the transition to a situation where hadronic internal degrees of freedom determine the interaction. The onset of the QCD scaling regime might take place in $pp \rightarrow \{pp\}_s \gamma$ at a beam energy $T_p \approx 2$ GeV, corresponding to the $E_\gamma \approx 1$ GeV which, it is suggested, is the start of the domain for deuteron photodisintegration [38].

Although the maximum proton beam energy at COSY is nearly 3 GeV, the identification of the $pp \rightarrow \{pp\}_s \gamma$ reaction through the pp missing mass becomes progressively harder as the energy increases, as is well illustrated by the data in figure 2. Therefore any attempt to use this reaction for the investigation of the γNN dynamics and its relation to the quark degrees of freedom would certainly necessitate the detection of the γ in coincidence. This is a challenge for the future.

Acknowledgments

The authors wish to thank other members of the ANKE collaboration for their help and assistance in the running of the experiment. We are grateful also to the COSY crew for providing good working conditions. Correspondence with Kanzo Nakayama has been very helpful. This work has been partially supported by the BMBF (grant ANKE COSY-JINR), RFBR (09-02-91332), DFG (436 RUS 113/965/0-1), the JCHP FFE, and the HGF-VIQC.

References

- [1] Laget J M 1989 *Nucl. Phys. A* **497** 391.
- [2] Arenhövel H *et al* 2003 *Modern Physics Letters A* **18** 190.
- [3] Leidemann W and Arenhövel H 1987 *Nucl. Phys. A* **465** 573.
- [4] Glistler J *et al* 2010 *Polarization Observables in Deuteron Photodisintegration below 360 MeV* arXiv:1003.1944.

- [5] Gilman R and Gross F 2002 *J. Phys. G: Nucl. Part. Phys.* **28** R37.
- [6] Audit G *et al* 1989 *Phys. Lett. B* **227** 331.
- [7] d'Hose N *et al* 1989 *Phys. Rev. Lett.* **63** 856.
- [8] Audit G *et al* 1991 *Phys. Rev. C* **44** R575.
- [9] Audit G *et al* 1993 *Phys. Lett. B* **312** 57.
- [10] Sarty A J *et al* 1993 *Phys. Rev. C* **47** 459.
- [11] Emura T *et al* 1994 *Phys. Rev. Lett.* **73** 404.
- [12] Tedeschi D J *et al* 1994 *Phys. Rev. Lett.* **73** 408.
- [13] Niccolai S *et al* 2004 *Phys. Rev. C* **70** 064003.
- [14] Pomerantz I *et al* 2010 *Phys. Lett. B* **684** 106.
- [15] Nefkens B M K *et al* 1979 *Phys. Rev. C* **19** 877.
- [16] Michaelian K *et al* 1990 *Phys. Rev. D* **41** 2689.
- [17] B.V. Przewoski B V *et al* 1992 *Phys. Rev. C* **45** 2001.
- [18] Yasuda K *et al* 1999 *Phys. Rev. Lett.* **82** 4775.
- [19] Huisman H *et al* 2002 *Phys. Rev. C* **65** 031001(R).
- [20] Mahjour-Shafiei M *et al* 2004 *Phys. Rev. C* **70** 024004.
- [21] Bilger R *et al* 1998 *Phys. Lett. B* **429** 195.
- [22] Komarov V *et al* 2008 *Phys. Rev. Lett.* **101** 102501.
- [23] Johansson A and Wilkin C 2009 *Phys. Lett. B* **673** 5; 2009 *Phys. Lett. B* **680** 111.
- [24] Barsov S *et al* 2001 *Nucl. Instrum. Methods Phys. Res. Sect. A* **462** 354.
- [25] Dymov S *et al* 2006 *Phys. Lett. B* **635** 270.
- [26] Arndt R A *et al* 2007 *Phys. Rev. C* **76** 025209; <http://gwdac.phys.gwu.edu>, SAID solution SP07.
- [27] Crawford R *et al* 1996 *Nucl. Phys. A* **603** 303.
- [28] Niskanen J A 2006 *Phys. Lett. B* **642** 34.
- [29] Wilhelm P, Niskanen J A, Arenhövel H 1995 *Phys. Rev. C* **51** 2841; 1995 *Phys. Rev. Lett.* **74** 1034.
- [30] Nakayama K and Haberzetti H 2009 *Phys. Rev. C* **80** 051001(R).
- [31] Nakayama K 2009 (private communication).
- [32] Uzikov Yu N 2009 *Proc. XIX Int. Baldin Seminar on High Energy Physics Problems (Dubna 2008)* vol 2 ed A N Sissakian *et al* (JINR, Dubna, Russia) 307.
- [33] Wiringa R B, Schiavilla R, Pieper S C, and Carlson J 2008 *Phys. Rev. C* **78** 021001.
- [34] Shneor R *et al* 2007 *Phys. Rev. Lett.* **99** 072501.
- [35] Subedi R *et al* 2008 *Science* **320** 1476.
- [36] Dymov S 2008 Institut für Kernphysik/COSY Annual Report, [\protect\vrule width0pt\protect\href{http://fz-juelich.de/ikp/anke/en/annual_reports/08/S.Dymov.pdf}](http://fz-juelich.de/ikp/anke/en/annual_reports/08/S.Dymov.pdf)
- [37] Kacharava A, Rathmann F and Wilkin C 2005 *Spin Physics from COSY to FAIR*, COSY proposal 152, arXiv:nuclex/ 0511028.
- [38] Rossi P *et al* 2005 *Phys. Rev. Lett.* **94** 012301.